

Electronic Supplementary Information

Tuning Molecular Adsorption in SBA-15-Type Periodic Mesoporous Organosilicas by Systematic Variation of their Surface Polarity

Hyunjin Moon^a, Songi Han^{*a,b}, Susannah L. Scott^{*a,b}

^aDepartment of Chemical Engineering, and ^bDepartment of Chemistry & Biochemistry, University of California, Santa Barbara, California 93106, United States.

*songihan@ucsb.edu, *sscott@ucsb.edu

Table of Contents		Page
Fig. S1	TGAs measured in air for various SBA-15-type PMO materials	S2
Table S1	Amounts of silane precursors used in the synthesis of various SBA-15-type PMO materials	S3
Fig. S2	SEM images of various SBA-15-type PMO powders	S4
Fig. S3	¹³ C CP/MAS NMR spectra of T25-B75, B75-BP25, and BP100 materials	S5
Fig. S4	Low-angle powder X-ray diffraction patterns of various SBA-15-type PMO materials	S6
Fig. S5	Wide-angle powder X-ray diffraction patterns for phenylene- and biphenylene-bridged SBA-15-type PMOs	S6
Fig. S6	N ₂ adsorption-desorption isotherms and pore size distributions for SBA-15-type PMO materials	S7
Table S2	Fluorescence maxima for Prodan adsorbed on various SBA-15-type PMO powders, both in the dry state, and suspended in water	S8
Table S3	Relative polarities of various solvents, and their Prodan emission maxima	S8
Table S4	Relative polarities of dry SBA-15-type PMO powders, and the powders suspended in water	S9
Scheme S1	Functionalization of silica with 4-carboxy-TEMPO radical	S9
Fig. S7	Continuous-wave EPR spectra of 4-carboxy-TEMPO-functionalized SBA-15-type PMO materials, suspended in water at 120 K	S10
Table S5	Amounts of <i>p</i> -cresol, phenol, and furfural adsorbed on various SBA-15-type PMO materials from water, DMSO, and benzene solutions	S11
	Additional references	S12

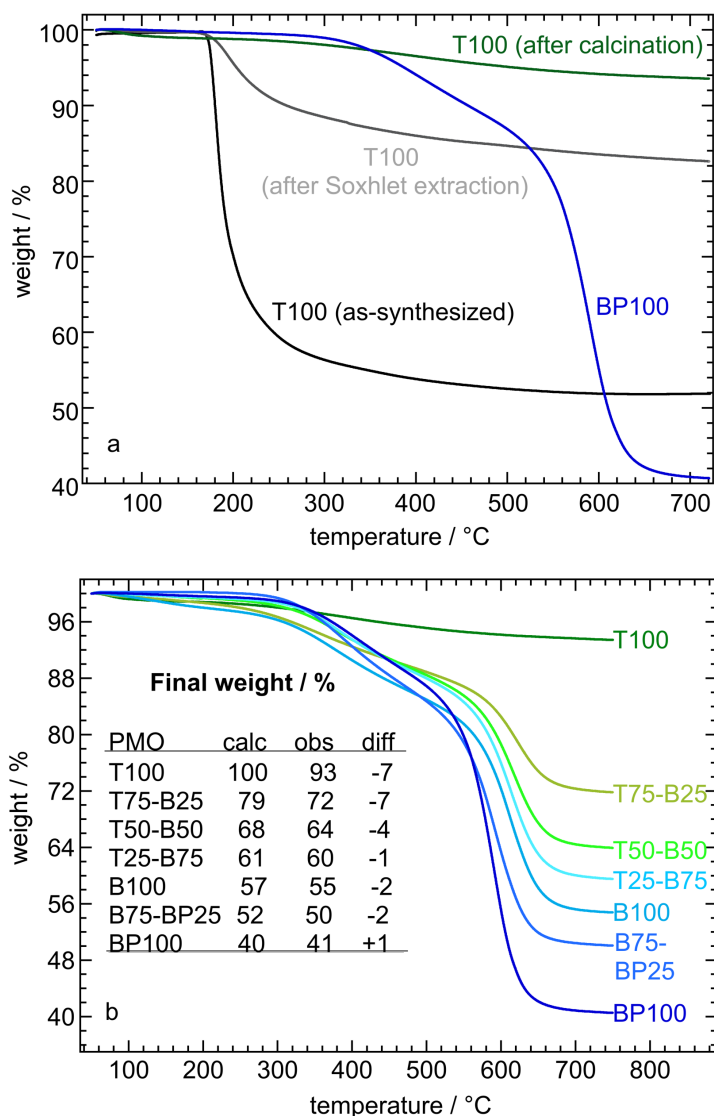


Fig. S1. TGAs measured in air for (a) T100: as-synthesized and after Soxhlet-extraction, as well as after calcination at 250 °C for 3 h; and BP100 (also after calcination at 250 °C for 3 h, blue); and (b) various PMOs after surfactant removal by Soxhlet extraction and calcination. All TGA data were recorded at a heating rate of 10 °C/min. The inset table shows the weight fraction of the inorganic component of each PMO (i.e., excluding phenylene and biphenylene bridging groups). Calculated values are based on the composition of the synthesis mixtures, using the formulas $m = x \text{ SiO}_2 + (1-x) \text{ O}_{1.5} \text{ SiC}_6\text{H}_4\text{SiO}_{1.5}$, and $m = y \text{ O}_{1.5} \text{ SiC}_6\text{H}_4\text{SiO}_{1.5} + (1-y) \text{ O}_{1.5} \text{ SiC}_{12}\text{H}_8\text{SiO}_{1.5}$, where x and y are the mol fractions of TEOS and BTEB, respectively. Observed values were obtained from the apparent weight losses, measured by TGA. The small differences are attributed to loss of water by surface dehydroxylation.

Table S1. Amounts of each silica precursor^a (mmol) used in the synthesis of various SBA-15-type PMO materials

Material	TEOS	BTEB	TEOS/BTEB ^b	BTEBP	BTEB/BTEBP ^c
T100	30.0	-		-	
T75-B25	12.6	4.2	3	-	
T50-B50	5.8	5.8	1	-	
T25-B75	2.2	6.6	1/3	-	
B100	-	7.2		-	
B75-BP25	-	5.5		1.8	3
BP100	-	-		6.5	

^a Tetraethyl orthosilicate (TEOS), 1,4-bis(triethoxysilyl)benzene (BTEB), 4,4'-bis(triethoxysilyl)-1,1'-biphenyl (BTEBP).

^b The optimal amounts of silane to form a single-component material using 3.0 g P123 are 30 and 7.2 mmol for TEOS and BTEB, respectively.^{1,2} For the two-component materials, the amount of TEOS decreases gradually from 30 to 0 mmol, while the amount of BTEB increases gradually 0 to 7.2 mmol. The amounts of TEOS and BTEB were chosen to give TEOS/BTEB ratios of 3, 1, and 1/3.

^c The amounts of BTEB and BTEBP used to synthesize B75-BP25 were determined in a similar fashion, based on the optimal amount of BTEBP needed.³

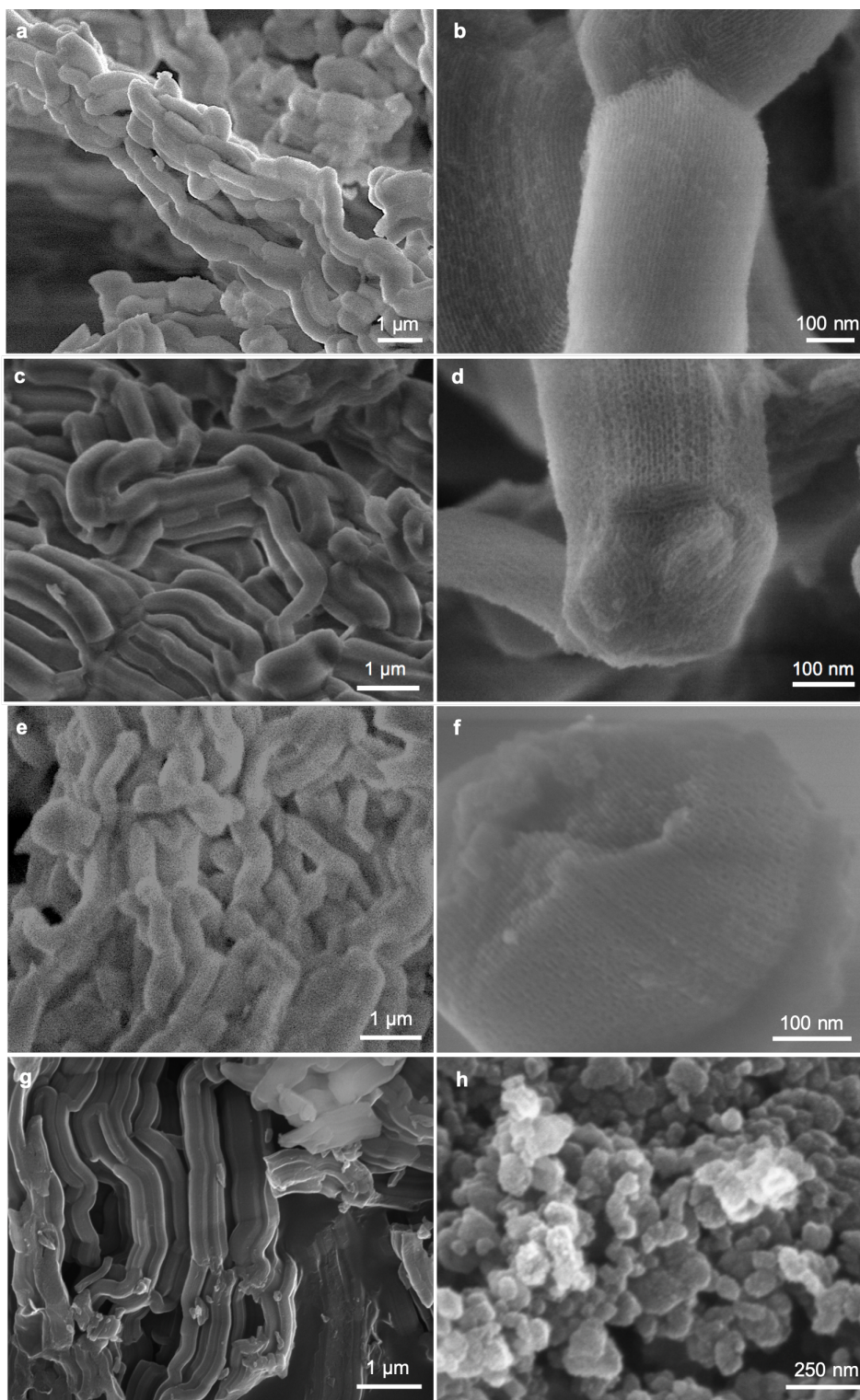


Fig. S2. SEM images of some SBA-15-type PMO materials: (a), (b) T100; (c), (d) T50-B50; (e), (f) B100; each presented at two different magnifications (at the higher magnification, pore openings are visible); as well as (g) B75-BP25; and (h) BP100.

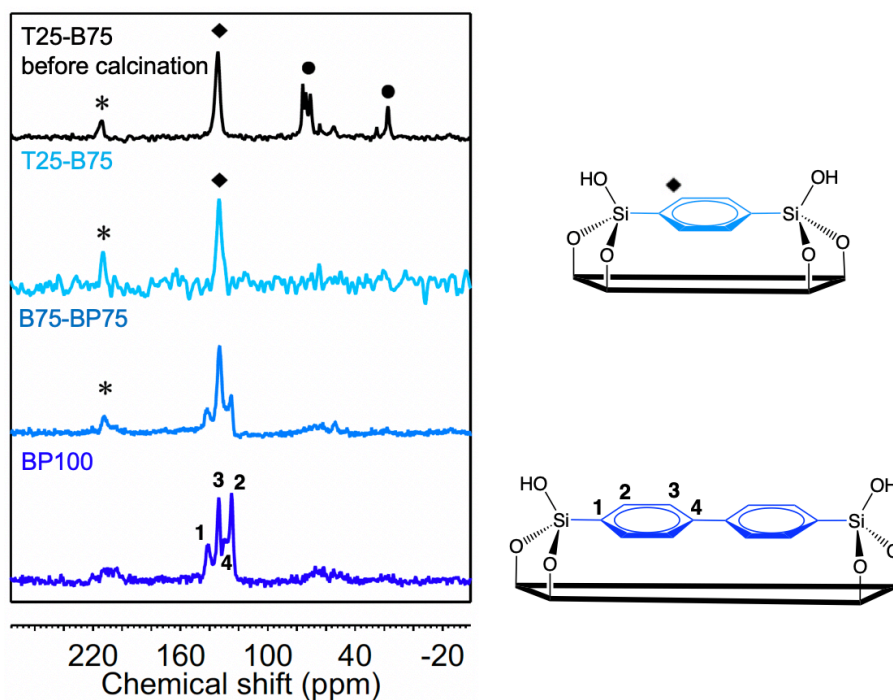


Fig. S3. ^{13}C CP/MAS NMR spectra of various SBA-15-type PMO materials (10 kHz MAS; * indicates a spinning side-band). Signals at 17 and 70-76 ppm in the spectrum of T25-B75 correspond to residual P123 surfactant (\bullet),⁴ which remains even after Soxhlet extraction with ethanol for 24 h. These signals disappear when the material is calcined in air at 250 °C for 3 h.² The remaining peak at 134 ppm corresponds to a single type of phenylene carbon.⁵ Signals at 125, 129, 134, and 141 ppm in the spectrum of BP100 correspond to the four chemically distinct biphenylene carbons.^{3,5} Signals for both phenylene and biphenylene groups are observed in the spectrum of B75-BP25.

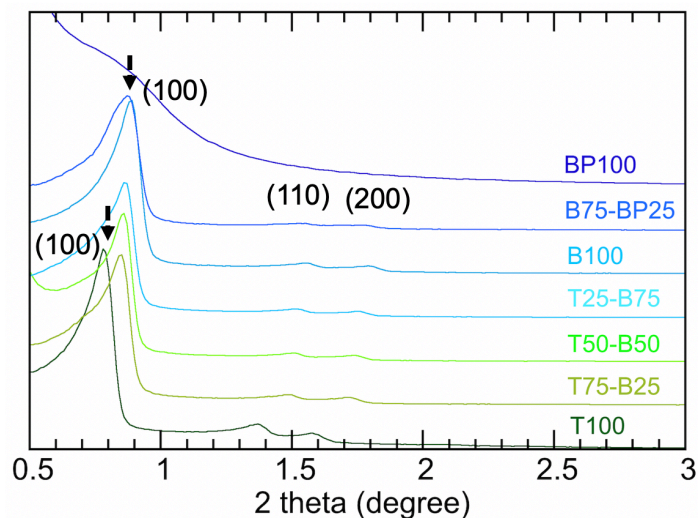


Fig. S4. Small-angle powder X-ray diffraction patterns of various SBA-15-type PMO materials. The location of the d_{100} reflection indicates the mesopore spacing.

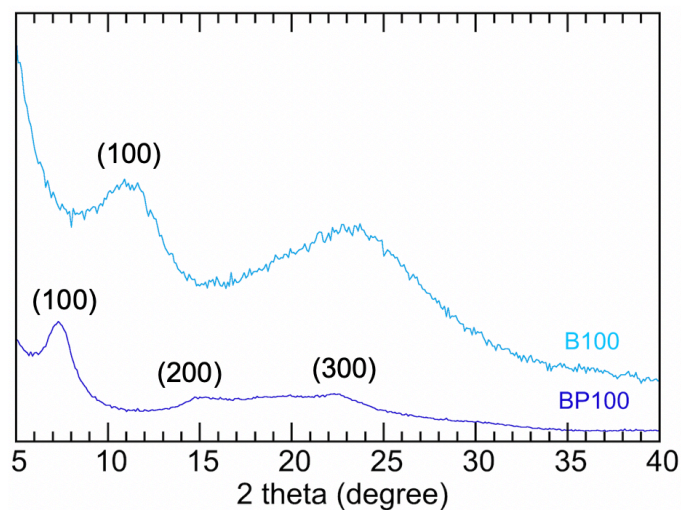


Fig. S5. Wide-angle powder XRD patterns for two SBA-15-type PMO materials. All peaks are relatively broad, typical of mesoporous silica synthesized using a non-ionic surfactant. The peak at $2\theta = 11^\circ$ for B100 corresponds to a phenylene d -spacing of 8.1 \AA .² For BP100, the peak at $2\theta = 7.3^\circ$ corresponds to a periodic biphenylene structure with a d -spacing of 11.9 \AA , and its higher-order reflections (14.7 and 22.3°).^{3,6}

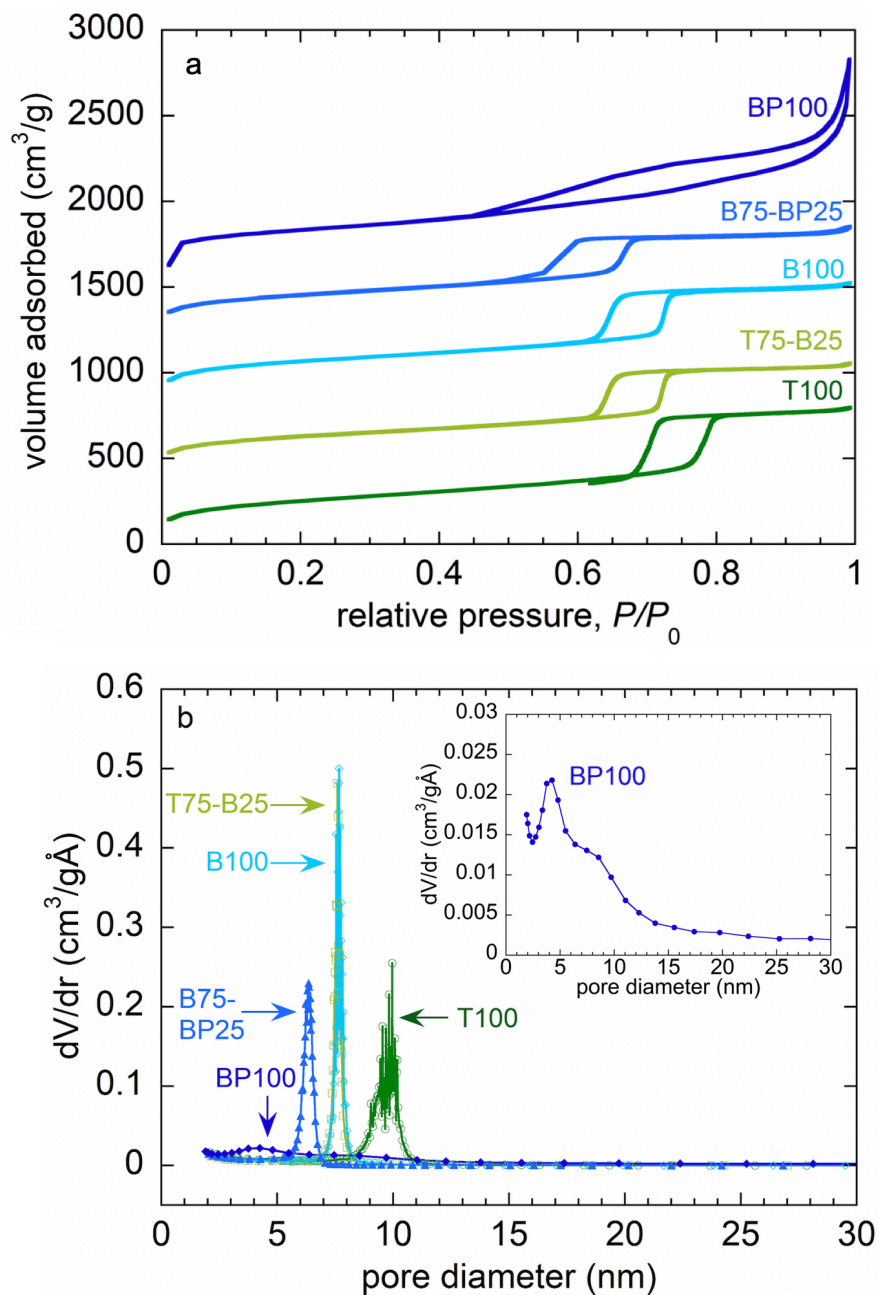


Fig. S6. (a) N_2 adsorption isotherms for PMOs. The data are offset vertically for clarity. All are type IV isotherms typical of mesoporous materials. For BP100, interparticle porosity causes the hysteresis loop to extend to very high relative pressures.³ Pore volumes measured at $P/P_0 = 0.95$ and 0.99 are 1.18 and 1.52 cm^3/g , respectively. (b) Pore size distributions for selected PMOs. The inset shows the pore size distribution for BP100.

Table S2. Fluorescence maxima (nm) for Prodan adsorbed on various SBA-15-type PMO powders, both in the dry state and suspended in water

Material	Peak position ^a	
	in water	dry
T100	526	509
T75-B25	512	499
T50-B50	510	494
T25-B75	507	493
B100	499	489
B75-BP25	490	480
BP100	482	473

^a The measurement error in the peak position is ± 1 nm.

Table S3. Relative polarities of various solvents, and their Prodan emission maxima (nm)

Solvent	Relative polarity ^a	λ_{max} ^b
water	1.000	527
methanol	0.762	502
ethanol	0.654	493
1-butanol	0.586	484
1-octanol	0.537	476
DMSO	0.444	465

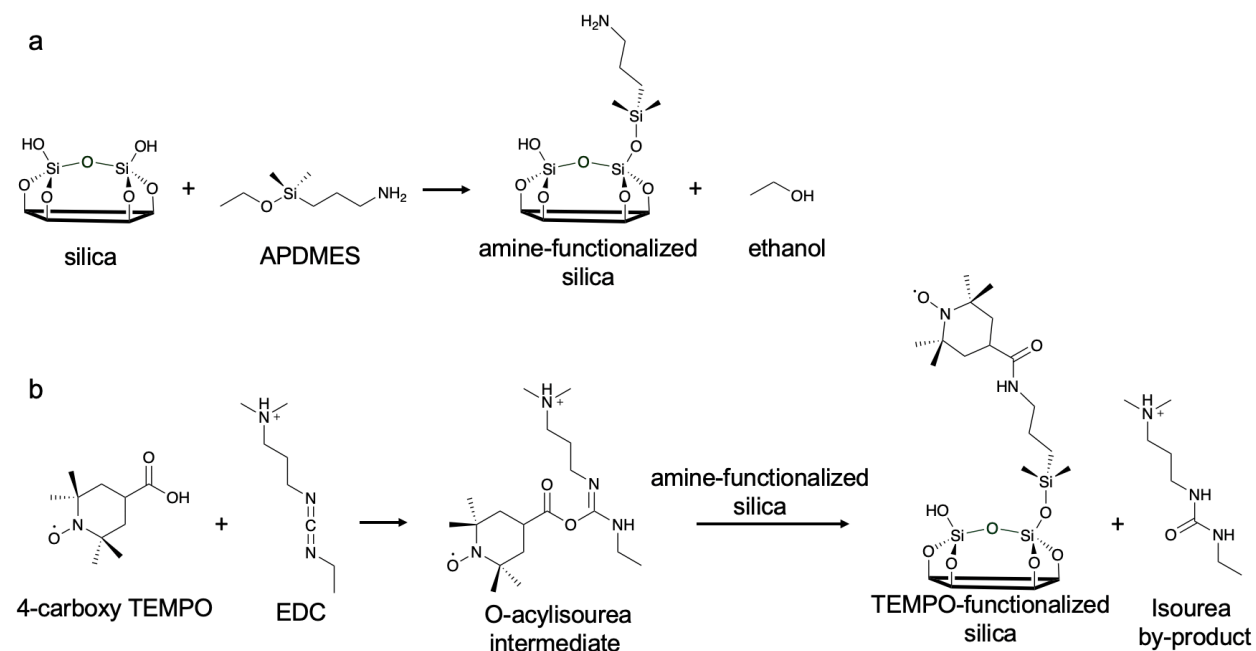
^a Inferred previously, by measuring the shift in the absorption spectrum of Reichardt's dye.^{7,8}

^b From a previous study.⁹

Table S4. Relative polarities of dry organosilica powders, and organosilicas suspended in water

Material	Relative <i>dry</i> surface polarity ^a	Relative <i>wet</i> surface polarity ^a
T100	0.81	0.99
T75-B25	0.71	0.86
T50-B50	0.67	0.82
T25-B75	0.66	0.79
B100	0.63	0.71
B75-BP25	0.55	0.64
BP100	0.50	0.57

^a Relative polarity was interpolated using the maximum fluorescence wavelength of adsorbed using a calibration curve based on the emission of Prodan in various solvents (Table S3).



Scheme S1. Procedure for functionalization of (organo)silicas with 4-carboxy-TEMPO radicals: (a) the surface is modified with aminopropyl groups by grafting APDMES ((3-aminopropyl)-dimethylethoxysilane) from a pH 7 buffer solution; (b) the tethered amine is modified with 4-carboxy-TEMPO, using EDC (*N*-(3-dimethylaminopropyl)-*N*-ethylcarbodiimide hydrochloride) to catalyze the reaction.

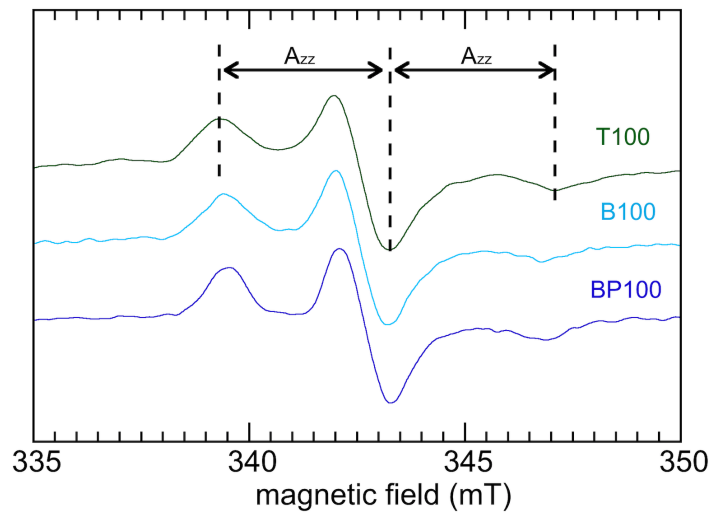


Fig. S7. Continuous-wave EPR spectra of 4-carboxy-TEMPO-functionalized SBA-15-type PMO materials, suspended in a frozen water solution at 120 K. The value of A_{zz} is defined as one-half the separation of the outer hyperfine extrema.¹⁰

Table S5. Adsorbed amounts (mmol/g) and standard deviations (SD) for 40 mM solutions of *p*-cresol, phenol, and furfural in water, DMSO, and benzene, on various PMOs ^a

Material	water						DMSO				benzene	
	<i>p</i> -cresol		phenol		furfural		phenol		furfural		furfural	
	adsorbed	SD	adsorbed	SD	adsorbed	SD	adsorbed	SD	adsorbed	SD	adsorbed	SD
T100	0.103	0.024	0.061	0.030	0.130	0.051	0.016	0.028	0	0	0.545	0.015
T75-B25	0.204	0.107	0.061	0.002	0.307	0.036	0.016	0.028	0.061	0.006	0.416	0.011
T50-B50	0.351	0.012	0.092	0.006	0.396	0.029	0.016	0.028	0.064	0.006	0.277	0.008
T25-B75	0.447	0.001	0.248	0.004	0.438	0.088	0.030	0.038	0.063	0.005	0.167	0.063
B100	0.539	0.026	0.364	0.034	0.442	0.037	0.058	0.051	0.092	0.028	0.042	0.072
B75-BP25	0.814	0.046	0.630	0.061	0.526	0.081	0.078	0.042	0.156	0.076	0.043	0.075
BP100	1.127	0.034	0.820	0.042	0.903	0.041	0.506	0.061	0.216	0.067	0.043	0.075

^a In each experiment, 20 mg PMO was combined with 1.5 mL solution at 296 K.

ADDITIONAL REFERENCES

- 1 D. Zhao, J. Feng, Q. Huo, N. Melosh, G. H. Fredrickson, B. F. Chmelka and G. D. Stucky, *Science*, 1998, **279**, 548–552.
- 2 Y. Goto and S. Inagaki, *Chem. Commun.*, 2002, 2410–2411.
- 3 Y. Yang and A. Sayari, *Chem. Mater.*, 2007, **19**, 4117–4119.
- 4 Y. Wang, B. Zibrowius, C. Yang, B. Spliethoff and F. Schüth, *Chem. Commun.*, 2004, 46–47.
- 5 Y. Yang and A. Sayari, *Chem. Mater.*, 2008, **20**, 2980–2984.
- 6 M. P. Kapoor, Q. Yang and S. Inagaki, *J. Am. Chem. Soc.*, 2002, **124**, 15176–15177.
- 7 C. Reichardt and T. Welton, *Solvents and Solvent Effects in Organic Chemistry*, Wiley-VCH: Weinheim, 2011.
- 8 C. Reichardt, *Chem. Rev.*, 1994, **94**, 2319–2358.
- 9 J. Catalan, P. Perez, J. Laynez and F. G. Blanco, *J. Fluoresc.*, 1991, **1**, 215–223.
- 10 M. B. McBride, In *Advanced Chemical Methods for Soil and Clay Minerals Research*. J. W. Stucki and W. L. Banwart, Eds. *NATO Sci. Ser. C, Vol. 63*, Springer: Dordrecht, pp. 423-450 (1980).